Diffusion of Extracellular K^+ Can Synchronize Bursting Oscillations in a Model Islet of Langerhans

Cynthia L. Stokes and John Rinzel
Mathematical Research Branch, National Institute of Diabetes and Digestive and Kidney Diseases, National Institutes of Health, Bethesda, Maryland 20892 USA

ABSTRACT Electrical bursting oscillations of mammalian pancreatic β-cells are synchronous among cells within an islet. While electrical coupling among cells via gap junctions has been demonstrated, its extent and topology are unclear. The β-cells also share an extracellular compartment in which oscillations of K^+ concentration have been measured (Perez-Armendariz and Atwater, 1985). These oscillations (1–2 mM) are synchronous with the burst pattern, and apparently are caused by the oscillating voltage-dependent membrane currents: Extracellular K^+ concentration (K_e) rises during the depolarized active (spiking) phase and falls during the hyperpolarized silent phase. Because raising K_e depolarizes the cell membrane by increasing the potassium reversal potential (V_K), any cell in the active phase should recruit nonspiking cells into the active phase. The opposite is predicted for the silent phase. This positive feedback system might couple the cells' electrical activity and synchronize bursting. We have explored this possibility using a theoretical model for bursting of β-cells (Sherman et al., 1988) and K^+ diffusion in the extracellular space of an islet. Computer simulations demonstrate that the bursts synchronize very quickly (within one burst) without gap junctional coupling among the cells. The shape and amplitude of computed K_e oscillations resemble those seen in experiments for certain parameter ranges. The model cells synchronize with exterior cells leading, though incorporating heterogeneous cell properties can allow interior cells to lead. The model islet can also be forced to oscillate at both faster and slower frequencies using periodic pulses of higher K^+ in the medium surrounding the islet. Phase plane analysis was used to understand the synchronization mechanism. The results of our model suggest that diffusion of extracellular K^+ may contribute to coupling and synchronization of electrical oscillations in β-cells within an islet.

INTRODUCTION

Pancreatic β-cells in islets of Langerhans exhibit characteristic oscillations in membrane potential in response to glucose and other insulin secretagogues (Dean and Matthews, 1970; for review see: Ashcroft and Rorsman, 1989; Atwater et al., 1989). This electrical burst pattern consists of hyperpolarized silent phases alternating with depolarized active phases during which fast action potentials ("spikes") occur (e.g., Fig. 2 illustrates a simulated burst pattern). The burst frequency is typically 2–6 min^{-1}, while spike frequency during the active phase is about 3–6 s^{-1} (Meissner and Schmelz, 1974). The onset of electrical bursting after glucose exposure occurs slightly before insulin secretion is observed, and the average spike rate correlates with insulin secretion level as glucose concentration is varied (Meissner, 1976a; for review see: Atwater et al., 1989).

Bursting appears to occur with near synchrony among the β-cells in an islet (Meissner, 1976b; Eddlestone et al., 1984; Meda et al., 1984). For most of the cycle, cells are together in either the active or silent phase, though transitions between the two phases may have lags of 1–2 s among cells (Eddlestone et al., 1984; Meda et al., 1984). Electrical coupling among the β-cells via gap junctions has been postulated as a mechanism by which the burst oscillations could be synchronized throughout an islet (Eddlestone et al., 1984; Mathias, 1985; Meda et al., 1986; Chay and Kang, 1988; Sherman et al., 1988), and theoretical studies lend support for the idea (Sherman et al., 1988; Sherman and Rinzel, 1991; Smolen et al., 1993). While the existence of gap junctions between β-cells is clear, the extent of electrical coupling throughout an islet remains uncertain. Lucifer yellow dye injected into single cells in an islet only spreads to a few nearby cells (Meda et al., 1986), suggesting the existence of small domains of gap-junctionally coupled cells. Perez-Armendariz et al. (1991) measured electrical coupling in 65% of cell pairs from freshly dispersed islets, though no dye transfer was observed in vitro. Unfortunately, these data do not demonstrate whether domains or a more diffuse gap junctional coupling exists in the intact islet.

A second possible mechanism of coupling, via "ionic interactions," is suggested by experiments of Perez-Armendariz and coworkers (Perez-Armendariz et al., 1985; Perez-Armendariz and Atwater, 1986). Using ion-sensitive electrodes, they measured oscillations in K^+ and Ca^{2+} concentrations in the extracellular space of the islet (K_e and Ca_e, respectively). Extracellular K^+ concentration varied by up to 2 mM over a resting concentration of 5 mM, while Ca_e varied by up to 1 mM below a baseline of 2.6 mM. These oscillations were synchronous with the burst pattern: K_e increased during the active phase and decreased during the silent phase, while Ca_e did the opposite. This is consistent with the increased efflux of K^+ and influx of Ca^{2+} during the active phase, leading to accumulation and depletion of the two ions, respectively, in the extracellular space. The oscillations in K_e

Received for publication 15 October 1992 and in final form 30 April 1993.

Address reprint requests to Cynthia L. Stokes. Present address: Department of Chemical Engineering, University of Houston, Houston, TX 77204–4792. Tel.: 713-743-4309; Fax: 713-743-4323; e-mail: stokes@jetson.uh.edu.

0006-3495/93/08/597/11 $2.00

are likely to have a significantly greater effect on membrane potential than Ca_e, because the membrane is significantly more permeable to K^+. In fact, the membrane potential approaches the K^+ reversal potential (V_K), about −75 mV, when the cells are not bursting (e.g., low glucose concentration in medium; Atwater et al., 1989). Hence, in this work we have focused solely on the effects of extracellular K^+. Because the extracellular space is shared among cells, efflux of K^+ from one cell should depolarize adjacent cells and, by diffusion, cells further away. The spiking of a cell would raise K_e, depolarize other cells, and recruit nonspiking cells to enter the active phase (by increasing their V_K) or keep other spiking cells in the active phase. These coupling effects might help to synchronize bursting among cells.

There is direct evidence that external K^+ has significant effects on the burst pattern. Exposing excised islets to step changes in K^+ concentration in the perifusion medium causes premature entrance to or exit from the active phase, depending on when in the burst period the change was made (Cook et al., 1981). Raising K^+ concentration also depolarizes the membrane, and the burst pattern is lost to steady depolarization between 8 and 15 mM potassium. Short pulses (2 s) of 10 mM K^+ in the perifusion medium with frequency higher than that of the normal burst rhythm can also force the islet to burst at the pulse frequency (C. L. Stokes, unpublished observations). Other cell types including neurons (for review see Sykova (1983)) and heart muscle (Kline and Morad, 1978) are sensitive to changes in external K^+ concentration, lending support to the hypothesis that K_e may have significant effects on electrical activity in the pancreatic islet.

In this paper we consider how the accumulation and diffusion of K^+ in the extracellular space affects the bursting of β-cells in an islet-like structure. Of particular interest is the ability of this ionic interaction alone to synchronize the burst pattern among β-cells. Here we define synchrony as one-to-one bursting, with all cells in the active or silent phase at (approximately) the same time. Chay and Keizer (1985) investigated the effect of K_e on β-cell burst oscillations using a theoretical model but did not consider how it might affect burst synchronization. Our mathematical model describes the bursting of individual β-cells within a three-dimensional structure through which extracellular K^+ can diffuse. The bursting of β-cells is described by a deterministic nonlinear model (Sherman et al., 1988), and the accumulation of K^+ is modeled with a reaction-diffusion equation. Our most significant result is that K^+ accumulation and diffusion can yield synchrony, even without electrical coupling. Step changes in and periodic pulses of K^+ affect bursting in the model similar to the experiments noted above.

2. MATHEMATICAL MODEL

2.1 Single β-cell burst model

The mathematical model which describes the electrical behavior of each β-cell comes from Sherman et al. (1988) as revised from Chay and Keizer (1983). Three nonlinear differential equations are needed for each cell. The first two equations describe action potentials generated by nonlinear voltage-dependent currents through K^+ and Ca^{2+} channels that are opposite in direction and offset slightly in time:

$$C_m \frac{dV}{dt} = -I_K - I_{Ca} - I_{K\text{-}Ca}$$

$$= -\bar{g}_K n(V - V_K) - \bar{g}_{Ca} m_\infty(V) h(V)\,(V - V_{Ca}) - \bar{g}_{K\text{-}Ca} \frac{Ca_i}{K_d + Ca_i}(V - V_K) \quad (1)$$

$$\frac{dn}{dt} = \lambda\left[\frac{n_\infty(V) - n}{\tau_n(V)}\right] \quad (2)$$

where V is the membrane potential; t is time; I_{Ca}, I_K, and $I_{K\text{-}Ca}$ are the currents for the voltage-dependent Ca^{2+} channel, delayed-rectifier K^+ channel, and Ca^{2+}-activated K^+ channel (K-Ca channel), respectively; $\bar{g}_{Ca}$, $\bar{g}_K$, and $\bar{g}_{K\text{-}Ca}$ are the total conductances per cell for these channel populations; and C_m is the total membrane capacitance. V_K and V_{Ca} are the K^+ and Ca^{2+} reversal potentials, respectively; the driving force for K^+ is $V\text{-}V_K$ and that for Ca^{2+} is $h(V)(V\text{-}V_{Ca})$, modified from Ohmic. Conductance of the K-Ca current is voltage-independent; it is activated instantaneously by intracellular free calcium (concentration = Ca_i) with K_d as the dissociation constant for Ca^{2+} binding to the channel. Gating properties of the other channels are described by $m_\infty(V)$, the steady state fraction of open, voltage-dependent Ca^{2+} channels, and $n(V,t)$, the fraction of open delayed-rectifier K^+ channels. For the latter channel, $n_\infty(V)$ is the steady state fraction of open channels; $\tau_n(V)$ is the time constant; and λ is a dimensionless parameter, analogous to the temperature correction factor in the Hodgkin-Huxley model (Hodgkin and Huxley, 1952), which was used to fine-tune the K^+ time constant (Sherman et al., 1988). The functional forms of $\tau_n(V)$, $n_\infty(V)$, $m_\infty(V)$, and $h(V)$ and the standard parameter values used appear in the appendix.

This model belongs to a class of models in which bursting is regulated by a single variable that changes slowly (compared to V and n) at the rate of bursting (Rinzel, 1985). This variable provides negative feedback to slowly activate an outward current or inactivate an inward current during the active phase. In the model of Sherman et al. (1988), intracellular calcium (Ca_i) feeds back slowly to activate the conductance of the K-Ca channel. The slow Ca_i dynamics are given by

$$\frac{dCa_i}{dt} = f(-\alpha I_{Ca} - k_{Ca} Ca_i) \quad (3)$$

where f represents the rapid buffering capacity of the cell for Ca^{2+}, equaling the fraction of total cytosolic Ca^{2+} that remains free, $0 < f \ll 1$; k_{Ca} is the removal rate constant for cytosolic Ca^{2+} (e.g., by sequestration and pumping); and α converts units of current to concentration ($\alpha = 1/[2\,V_{cell}\,F]$, where V_{cell} is cell volume and F is Faraday's constant).

This is not the only possibility for the slow process. Others proposed include slow calcium inactivation of a calcium channel (Chay, 1987; Plant, 1988), ATP-modulation of the

ATP-dependent K^+ channel (Ashcroft et al., 1984; Cook and Hales, 1984; Keizer and Magnus, 1989; Smolen and Keizer, 1992), and slow voltage inactivation of a calcium channel (Satin and Cook, 1989; Hopkins et al., 1991; Smolen and Keizer, 1992). Note, in the latter two, Ca_i is not a slow variable. These models all conform to a similar mathematical structure for bursting, although they rely on different biophysical mechanisms. Each generates significant K^+ currents and is affected by changes in K_e and is therefore susceptible to K_e-coupling.

The mechanism for bursting in this model has been described in detail elsewhere (Rinzel, 1985; Sherman et al., 1988). Mathematically, we can view this behavior in the V-Ca_i phase plane, first considering Ca_i as a parameter since it varies slowly (Fig. 1). The dependence of the steady state potential on Ca_i is summarized by the Z-shaped curve, representing the faster spike-generating subsystem (Eqs. 1–2). The membrane potential is bistable for Ca_i between the "left knee" of the Z-curve at Ca_v and the point where the oscillation on the upper branch (labeled "osc") collides with the threshold state (middle branch of Z, unstable) at Ca_{HC}. The curve labeled "burst" illustrates how the membrane potential alternately tracks the hyperpolarized steady state (lower branch) and the depolarized oscillatory state (upper branch) during the silent and active phases, respectively, as Ca_i varies slowly back and forth between Ca_v and Ca_{HC}. See Fig. 2 *A* for a typical burst pattern. During the active phase Ca_i slowly increases and activates $I_{K\text{-}Ca}$. This causes the threshold voltage to rise slowly until it meets the spiking membrane potential to end the active phase. During the silent phase, Ca_i and $I_{K\text{-}Ca}$ decrease, causing a slow depolarization. When the membrane potential meets the slowly falling threshold the active phase begins anew. The time scale of calcium dynamics determines the burst period, hence the period varies inversely with f.

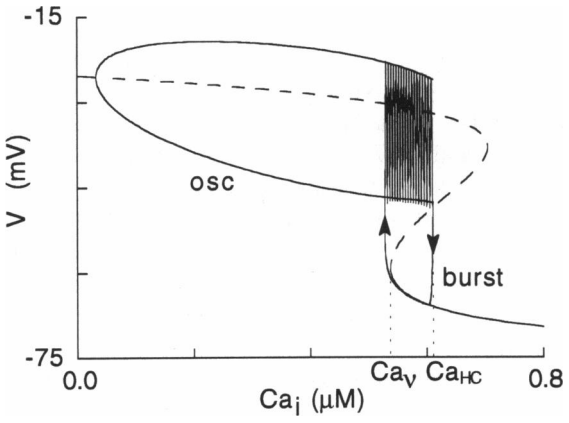

FIGURE 1 Solution structure of spike-generating subsystem, Eqs. 1–2. Membrane potential is plotted as a function of Ca_i, where Ca_i was treated as a parameter; computed using the program AUTO (Doedel, 1981). The Z-shaped curve represents the steady state voltage. Solid curves, stable steady states; dashed curves, unstable steady states. On the Z-curve, the depolarized steady state (upper branch) is unstable for a range of Ca_i values and is surrounded by a stable oscillation (labeled *osc*); the fork on this branch indicates the maximum and minimum voltages of this periodic, repetitive firing solution as a function of Ca_i. The left knee of the Z-curve at Ca_v is where the hyperpolarized steady-state (lower branch) joins the threshold saddle branch (middle branch). The upper, stable oscillation branch terminates at Ca_{HC} where the oscillating voltage collides with the saddle branch to form a homoclinic orbit and then disappears. A burst solution (labeled burst) is projected into this plane, superimposed on the bifurcation diagram (see Fig. 2 for a typical burst time course). Parameter values used are in the Appendix.

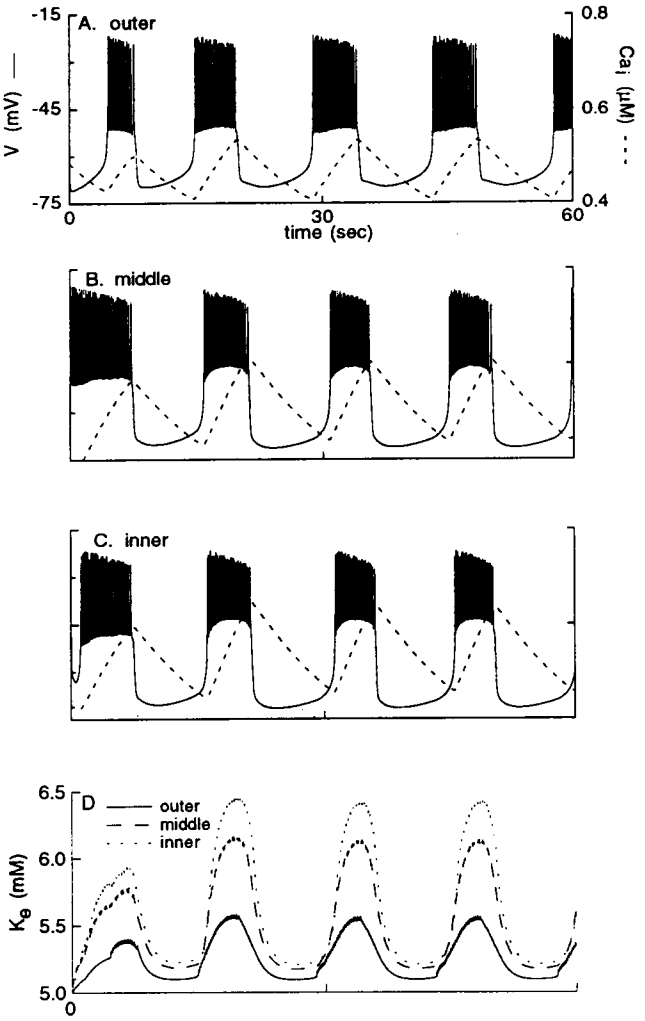

FIGURE 2 Bursting in cells at different locations in the spherical model islet. Membrane potential V and intracellular Ca^{2+} concentration Ca_i are illustrated for the outer-most bursting cell (two layers on the islet periphery are inactive) (*A*), the cell at $R/2$ (*B*), and the center cell (*C*). The scales on *A*–*C* are all as shown in *A*. (*D*) Extracellular potassium concentration (K_e) at the locations in *A*–*C*. The largest oscillations occur at the center of the islet, while the smallest are near the exterior.

2.2. K^+ diffusion model

Our model islet is formulated as follows. Individual β-cells reside in concentric shells of a sphere, much like the layers of an onion. The outermost layers in the model (two unless specified otherwise) do not burst. This is specified because β-cells occupy the core of an islet, with several layers of nonbursting cells (predominantly α-cells) forming the outermost layers (Bonner-Weir, 1988). The consequences of this choice are examined below. The cells' K^+ currents are treated as point sources of K^+ in the extracellular volume, with the

total current from a cell concentrated at the grid point corresponding to that cell's shell. The extracellular volume is treated as a continuous homogeneous medium for calculating K^+ diffusion, using an effective diffusion coefficient to account for the true heterogeneity of the extracellular space. The effective diffusion coefficient, D, was estimated (Perez-Armendariz et al., 1985) to be 0.9×10^{-5} cm^2/s, about half that for K^+ diffusion in water (1.83×10^{-5} cm^2/s (Robinson and Stokes, 1959)). The extracellular space is continuous with the medium outside the islet where K^+ concentration (K_{bath}) is constant.

For the model islet, the distribution of extracellular K^+ satisfies the reaction-diffusion partial differential equation

$$\frac{\partial K_e}{\partial t} = D\frac{1}{r^2}\frac{\partial}{\partial r}\left(r^2\frac{\partial K_e}{\partial r}\right) + \frac{1}{Fv_e}(I_K + I_{K\text{-}Ca}) \qquad (4)$$

where v_e is the volume of extracellular space per cell, and r is radial position. The first term on the right-hand side represents the diffusion of K^+ in the extracellular space, and the second term represents the K^+ currents through the cell membranes as given in Eq. 1. Because K_e varies, the reversal potential of K^+ (V_K) for all cells, assumed given by the Nernst potential, depends on the local value of K_e:

$$V_K(K_e) = \frac{F}{RT}\ln\left(\frac{K_e}{K_i}\right). \qquad (5)$$

K_i is the intracellular K^+ concentration, R the gas constant, and T the absolute temperature. For boundary conditions on K_e, we assume that the concentration at the circumference of the islet is constant at K_{bath} (e.g., the concentration in the perifusion medium in an excised islet experiment) and that there is no flux at the center of the islet ($\nabla K_e = 0$).

For this model islet, we assume spherical symmetry of the solution and compute diffusion only in the radial direction. This reduces the number of spatial dimensions from three to one. The calculated burst pattern of one cell in a shell represents the burst pattern of all cells in the shell. This symmetry assumption does not allow possible asymmetric solutions. In further calculations, however, we permitted lateral diffusion in two- and three-dimensional configurations (squares and cubes). These simulations resulted in symmetrically synchronized behavior, even for randomized initial conditions, supporting our symmetry assumption in the spherical islet calculations.

For numerical integration, Eqs. 1–4 were discretized in space and time. Time evolution of Eqs. 1–3 was done by a predictor-corrector method with a convergence criterion of 10^{-7} for relative differences between iterations. Calculation of the spatial profile from Eq. 4 at each time was simplified by offsetting the time step for this equation by one-half time step from that of Eqs. 1–3. This makes Eq. 4 linear, because the ionic current terms at each step are now treated as constants equal to those calculated from Eqs. 1–3 at the previous half time step. A tridiagonal matrix was solved to obtain the spatial solution for K_e at each time step. The spatial step size was 10 μm, the thickness of a model β-cell layer. The temporal step size was 0.1 ms. Halving this gave results that were indistinguishable from those using 0.1 ms. A singularity in the spherical diffusion operator at $r = 0$ was avoided by using the transformation $K^* = K_e r$ during the calculations; the boundary condition at $r = 0$ becomes $K^* = 0$. The calculations were performed on a Vax 8650 or Cray XMP programmed in FORTRAN 77. The standard parameter values used for the calculations are given in the Appendix.

3. RESULTS

3.1 Synchronization of bursting

When the three-dimensional spherical islet model is simulated with the cells initialized at random phases in their burst cycle, the cells quickly synchronize after about one burst (Fig. 2). In this spherically symmetric geometry, the outer cells always lead the transitions at steady bursting, entering the active or silent phase several seconds before the interiormost cells do. The lead is shorter at the transition from active to silent phase. These phase lags are similar to those measured by Eddlestone et al. (1984) in intact islets, though they found that either interior or exterior cells could lead (personal communication with I. Atwater, regarding Eddlestone et al. (1984)).

Extracellular K^+ oscillations are largest in the center of the islet and decrease toward the exterior (Fig. 2 *D*), as expected for diffusion in a sphere with a sink at the outside (the bath with constant K^+ concentration K_{bath}). These K_e oscillations are similar qualitatively to those measured experimentally (Perez-Armendariz et al., 1985; Perez-Armendariz and Atwater, 1986). Even though K_e has a time scale intermediate to those of V and Ca_i (see below), its time course is smoother because of diffusive coupling. Notice that K_e in the islet interior reaches a maximum before the end of the active phase, similar to some experimental records (Perez-Armendariz and Atwater, 1986), because the diffusional forces become larger than the K^+ membrane currents near the end of a burst. In addition, exterior cells have left the active phase, ceasing to supply K^+, and the rate of spiking decreases as the active phase proceeds (see Fig. 1). The K_e profile as a function of islet radius is approximately parabolic (not shown).

The lag-times among cells at the transitions between active and silent phases occur because of K_e gradients in the islet, and result in shorter active phases for interior cells. While the difference is slight in Fig. 2, it becomes more pronounced as the percent active phase is increased by, say, raising k_{Ca}. The Ca_i oscillations are also larger and reach a higher peak value in interior cells (Fig. 2, *A–C*). This occurs because the interior cells are more depolarized, resulting in a greater influx of Ca^{2+} even though the spike amplitude is generally larger in exterior cells. Because Ca_i is an important second messenger for insulin secretion (Wollheim and Sharp, 1981; Prentki and Wollheim, 1984), the increase in Ca_i caused by increased V_K might be important for secretion.

Variations in K_e at different depths in the islet also modulate burst shape (Fig. 2). The interior cells are more depo-

larized in the active phase, and the spikes are smaller and more frequent. The plateau potential on which the spikes ride can rise or fall, or rise then fall, depending on cell location. Varying parameters to increase K_e can result in other burst shapes as well, such as active phases with no spikes near the end (not shown). These results suggest that different K^+ concentrations and oscillation amplitudes might contribute to the variations in burst shapes observed experimentally.

For computational economy, the simulations in Fig. 2 do not conserve K^+ in a cell or within the islet. Test simulations including an ion pump that returns K^+ to the cells' interiors revealed no sacrifice of the synchronizing behavior (not shown). The K_e oscillations (e.g., Fig. 2 *D*) were shifted downward but synchronization was not affected. Since the cells lose only a small amount of K^+ per burst cycle, the rate of pumping needed for K^+ restoration is slow and longer integration times are needed to achieve steady state bursting.

3.2 Mechanism of synchronization

We apply phase plane methods to explore the synchronization mechanism. Considering K_e as a parameter, two parameter variation in AUTO (Doedel, 1981) reveals that the Ca_i thresholds for transitions between active and silent phases increase with K_e: in Fig. 3 *A*, the Ca_v and Ca_{HC} curves have positive slopes. We view the burst dynamics through cells' trajectories in the plane of the two slow variables, Ca_i and K_e (Fig. 3). Biophysically, this can be understood as follows. Increasing K_e leads to depolarization. The slow feedback process which underlies bursting compensates by shifting to a different operating range to exert a more hyperpolarizing influence. In our case, this means higher values of Ca_i and thus greater calcium-activated K^+ current.

An idealized view of synchronization (Fig. 3 *B*) is to imagine that near the end of the silent phase all cells are in "lockstep" (with identical K_e and Ca_i), and K_e is low, approximately equal to K_{bath}. All cells leave the silent phase simultaneously when Ca_i decreases to Ca_v (point *a* in Fig. 3 *B*). In the active phase, a nonuniform spatial distribution of K_e develops (points *b* in Fig. 3 *B*), with K_e largest in the center of the islet (as in Fig. 2 *D*). The cells' Ca_i-K_e trajectories now move rightward. The nonuniform K_e causes cells at different locations to have different active to silent phase transition thresholds; interior cells have larger values of Ca_{HC} and thus longer active phases (points *c* in Fig. 3 *B*). The exterior-most cell reaches its Ca_{HC} transition value first and re-enters the silent phase, its nearest interior neighbor does so next, and so on, until all cells have re-entered the silent phase (transition *c* to *d* in Fig. 3 *B*). K_e now decreases to a nearly uniform value across the islet (points *d* in Fig. 3 *B*) so that the next threshold Ca_v will be about the same for all cells (again, point *a* in Fig. 3 *B*). Because the interior cells left the active phase at higher values of Ca_i, they now have longer silent phases because their Ca_i's must decrease to the same Ca_v (point *a*) to re-enter the active phase. This idealized view results in longer expected active and silent phase durations for interior cells compared to more exterior cells, suggesting that cells in an islet cannot execute burst cycles in one-to-one synchrony.

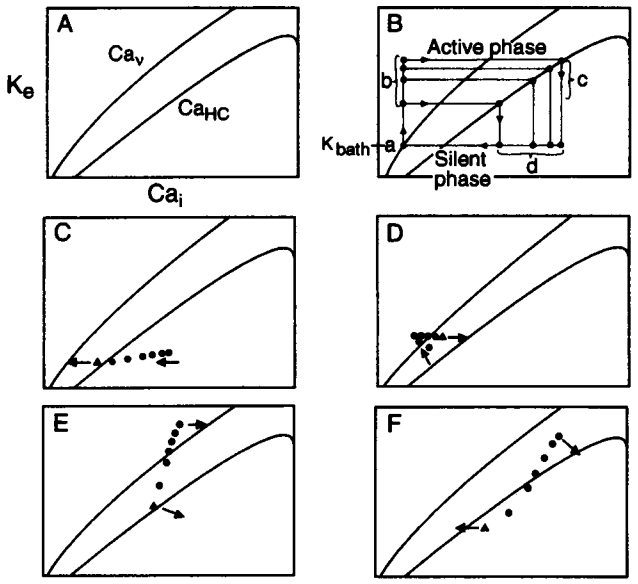

FIGURE 3 (*A*) Dependence of burst transition threshold points, Ca_v and Ca_{HC}, on K_e (equivalently, V_K by Eq. 5). Ca_v represents the left knee and Ca_{HC} the homoclinic point in Fig. 1, which vary with K_e. The axes in *A–F* are all as labeled in *A*. (*B*) Idealized view of Ca_i-K_e burst trajectories superimposed on the transition threshold curves from *A*. See Section 3.2 for explanation. (Point *a*) Ca_v for silent to active phase transition for all cells; (points *b*) Ca_i-K_e locations of cells immediately after that transition; (points *c*) Ca_{HC} values for transition from active to silent phase; (points *d*) Ca_i-K_e locations of cells immediately after that transition. (*C–F*) Actual simulated Ca_i-K_e trajectories for the spherical model islet superimposed on the transition threshold curves. The outermost bursting cell is denoted by a triangle, with the other cells as circles. Arrows indicate the "direction" in which the outermost and innermost cells are moving in the plane. (*C*) All cells in the silent phase. The outermost bursting cell (*triangle*) is furthest to the left and is approaching the Ca_v curve, at which it will switch to the active phase. (*D*) All but the innermost cell have crossed the Ca_v curve, entering the active phase. (*E*) All cells are in the active phase. The trajectories now move rightward and upward as Ca_i increases and K_e accumulates. (*F*) The outer cells reach the active to silent phase transition threshold, Ca_{HC}, first and re-enter the silent phase. Here, three cells have re-entered the silent phase. K_e decreases for all cells because of the decreased K^+ efflux from the outer cells. A later time point when all cells have re-entered the silent phase and K_e has decreased is shown in *C*.

What adjustments are made, then, to overcome the anticipated differences in active and silent phase durations so that cells can all oscillate with the same period and in synchrony? An important factor is the exterior boundary condition which requires that K_e for the outermost cells can vary only slightly from K_{bath}. In a synchronized islet, the outer cells' frequency is essentially determined by K_{bath}, and therefore these outer cells (expected to be "faster") must recruit the inner cells to shorten their periods. This occurs by diffusional coupling through K_e, which alters the cell trajectories and the transition points along the Ca_v and Ca_{HC} threshold curves from the preceding idealized view. We can visualize the mechanism by following the simulated trajectories of all bursting cells in Fig. 3, *C–F*.

In Fig. 3 *C* all cells are in the silent phase with the outermost cell just ready to become active. When this outermost cell depolarizes to enter the active phase, its efflux of K^+ increases, raising K_e locally and, by diffusion, throughout the islet (Fig. 3 *D*). This raises V_K and hence raises the Ca_ν threshold for more interior cells, even though those cells are still silent. This causes interior cells to enter the active phase earlier than expected. Each additional cell entering the active phase further raises K_e and hence Ca_ν, further shortening the silent phase of the remaining interior cells. When all cells are in the active phase the Ca_i-V_K trajectories move rightward in the Ca_i-V_K plane (Fig. 3 *E*). Because Ca_ν and Ca_{HC} threshold curves have positive slopes, the outer cell reaches its Ca_{HC} first and re-enters the silent phase (Fig. 3 *F*). Potassium efflux from this cell layer greatly diminishes, lowering K_e locally and, by diffusion, throughout the islet. Hence, the Ca_{HC} values that more interior cells must reach are smaller than anticipated, and their active phases are cut short. Each additional cell entering the silent phase causes K_e to further decrease everywhere, lowering the Ca_{HC} and shortening the active phase of other cells remaining in the active phase.

The net result is a positive feedback system among the cells; any cell making either transition recruits additional cells to that transition through diffusional coupling. The positive feedback not only equalizes burst period among cells, but also results in approximate phase synchrony, with all cells in the active or silent phase (nearly) simultaneously. We note that an additional compensating factor for equalizing the burst periods of cells is that Ca^{2+} influx is greater for inner cells due to their greater depolarization, also acting to shorten their anticipated active phase durations. This factor also explains why inner cells have a lower percentage active phase than outers.

The outer cells lead in the spatiotemporal burst pattern because the difference between Ca_ν and Ca_{HC} is less for them than for the inner cells, so their expected periods are shorter. Since their frequency is essentially determined by K_{bath}, these faster cells become the leaders; transitions occur in an orderly sequence with each cell following its nearest outer neighbor (Figs. 3, *C–F*). Burst order again reflects the significant role played by the boundary condition at the islet's periphery. If interior cells were intrinsically faster (say, because of different properties), burst order in a synchronized islet might be different; the period of bursting, however, would still be dominated by the outside cells (illustrated below in Section 3.5).

The above discussion implicitly assumes that diffusion of extracellular K^+ is adequately fast relative to Ca_i dynamics. If not, then the K_e-mediated period-shortening effects cannot compensate quickly enough and loss of synchrony may occur.

3.3. Loss of synchronization

As parameters are tuned so that frequency increases just beyond the regime for synchrony, arrhythmia emerges with most of the islet remaining synchronized except for the outermost cell layer. This outer layer bursts at a rate faster than the interior cells can follow. The phase lead of outer cells increases over several cycles until these cells burst twice, while the rest of the islet bursts only once (Fig. 4). These "extra bursts" occur more frequently as the causative parameter is changed further from the synchronized regime. At some value, the next most exterior cell also "breaks away," and so on. This onset of arrhythmia is determined by the relative rates of Ca_i and K_e. To maintain synchrony (1:1 bursting) potassium diffusional coupling must be sufficiently faster than Ca_i kinetics to ensure recruitment of inner cells by outers at each phase transition.

Increasing burst frequency by increasing the parameter f destroys synchrony (Fig. 4). Diffusion to the bath cannot deplete K^+ during the silent phase before the exterior cells re-enter the active phase and K^+ efflux begins again. For all other parameters constant (k_{Ca} such that active phase percent is about 30%, a commonly observed value), synchrony is lost at about $f = 0.00275$. This corresponds to a burst frequency of about 7 min^{-1}, faster than is usually observed in experiments. Smaller active phase percentages (smaller k_{Ca}) result in less accumulation of K^+, delaying the onset of arrhythmia as f is increased. Hence, k_{Ca} modulates the effect of changing burst frequency through f. Other parameters that lead to asynchrony are mentioned in Section 3.4.

Another important case involves our model's nonbursting cell layers around the exterior of the islet. This construct ensures that all β-cell layers synchronize for this islet size. For our standard parameter values, if the nonbursting layers are allowed to burst, they cycle too fast and cannot entrain the interior cells in 1:1 bursting. Changing the boundary condition from a constant K_{bath} to an unmixed fluid boundary layer around the islet (Perez-Armendariz et al., 1985) can substitute for the inactive cell layers and allow synchronization (not shown). The outer cells then also participate in K_e

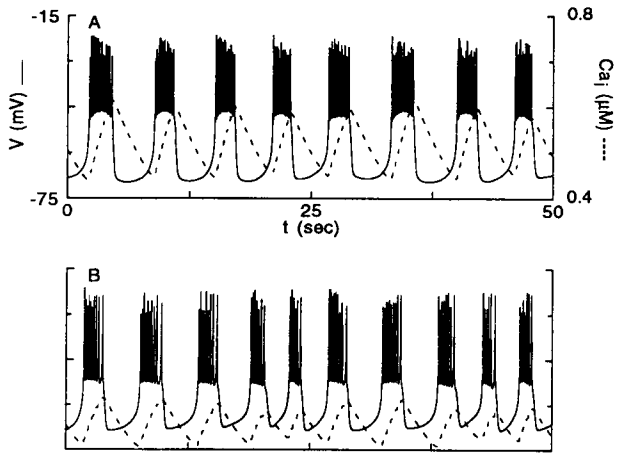

FIGURE 4 The onset of arrhythmia in the islet caused by increasing f to 0.0035. The outermost bursting cell has additional bursts, while the rest of the cells remain in one-to-one synchrony. (*A*) The cell in the center of the islet. All cells but the outermost burst in one-to-one synchrony with this cell (not shown). (*B*) The outermost bursting cell. Note that this cell bursts five times for every four bursts by the cell in the center (*A*). The scales in *A* and *B* are the same.

oscillations; their burst period is lengthened and they can again entrain interior cells in 1:1 bursting.

3.4. Parameter dependence of results

To describe the influence of various parameters, we identify three parameter groupings. They characterize 1) the fast, spike-generating ionic currents, 2) the slow processes for burst modulation in individual cells (calcium-handling in our case), and 3) the structural-transport properties which determine ionic intercellular coupling. Here, we fix parameters in the first group (see Appendix) to focus on parameters related to calcium-handling (f and k_{Ca}) and to coupling (R, D, v_e, and K_{bath}), which determine the dynamics of the two slower variables, Ca_i and K_e, respectively. The interaction of these two variables establishes the macroscopic spatiotemporal rhythm. Alternative spike-generating currents and slow burst-modulation mechanisms could be considered but synchronization by extracellular diffusion should still be modulated primarily by parameters in the negative-feedback loop for bursting (Ca_i) and in the positive-feedback loop for coupling (K_e).

3.4.1 Calcium-handling parameters

The burst frequency and percent active phase are determined by f and k_{Ca}, respectively. In experiments, as glucose concentration increases, active phase percent and duration increase monotonically, while burst frequency increases then decreases (Atwater et al., 1989; Dean and Matthews, 1970; Meissner and Schmelz, 1974). By comparison, varying f and k_{Ca} may be interpreted as changing calcium-buffering capacity and glucose concentration, respectively (Chay and Keizer, 1983). In our islet simulations, these parameters also modulate the size and shape of K_e oscillations, and in limiting regimes can affect burst synchronization as explained in Section 3.3.

For large enough k_{Ca} values, periodic bursting is replaced by continuous spiking. In an isolated cell model (Eqs. 1–3), the transition from bursting to continuous spiking occurs over a small range of k_{Ca} values near 0.045 s^{-1} (with constant K_e = 5 mM) through a sequence of complex, possibly chaotic, dynamic patterns (Chay and Rinzel, 1985; Rinzel, 1985). In the islet model, bursting gives way to continuous spiking around k_{Ca} = 0.059 s^{-1}, with a greater active phase percentage than for the isolated cell. The extended bursting regime is caused by dynamic changes in K_e that modulate Ca_v and Ca_{HC} (Fig. 3). The spatiotemporal pattern in the islet model is modified in the transition range (e.g., inner cells might lead, or remain bursting while outers spike continuously).

Regarding modulations of K_e, the amplitude of the K_e oscillations increases as the active phase duration increases. This occurs when either the active phase percent is increased (by raising k_{Ca} with f constant) or when the burst period is increased (by decreasing f with k_{Ca} constant). The shape of K_e oscillations is also modulated. The relative rates of K^+ diffusion and K^+ efflux determine whether or not K_e varies monotonically during the active phase or silent phase. If the active phase is long (k_{Ca} large), K_e may begin to decrease before the phase ends (see Fig. 2 *D* and Section 3.1). If the silent phase is long enough, K_e will begin increasing before the end (also seen in Fig. 2 *D*).

3.4.2 K_e-handling parameters

The ratio of islet radius squared to effective diffusion coefficient, R^2/D, affects the magnitude of K_e oscillations. Dimensional analysis shows that increasing D is equivalent to decreasing R^2 proportionally while maintaining a constant number of K^+ sources (β-cells) in that R. In reality, a larger islet would mean an increased number of β-cells at fixed density of one cell layer per 10 μm in radius, increasing the effect of R relative to that of D. That notwithstanding, increasing R^2/D increases the magnitude of K_e oscillations. This increase also affects the shape of the oscillations since greater accumulation of K_e during the active phase requires more time for dissipation during the silent phase. Burst synchronization is unaffected for a large range of values of R^2/D. For a given R, increasing D 10-fold does not destroy synchrony, although the K_e oscillations are reduced to about 0.1 mM and the transient approach to synchrony for random initial phase is much longer. Decreasing D too much leads to asynchrony through the same mechanism described in Section 3.3 for increasing f. For the standard islet configuration and parameters, this occurs at $D = 0.8 \times 10^{-5}$ cm^2/s. Varying R^2 rather than D gives equivalent effects, except that addition of cells (K^+ sources) along with increasing R causes breakaway at smaller R than predicted by the same value of R^2/D.

Our present solutions are limited to small to medium-sized islets ($R \leq 100$ μm for the standard parameter set) because of limitations of the underlying β-cell model (not the synchronization mechanism). If K_e, and hence V_K, becomes too great, spiking in the active phase disappears in the single cell model (Eqs. 1–3), leaving a slow square wave with a steadily depolarized active phase. This limit of around 7 mM is lower than observed experimentally, where bursting is replaced by constant depolarization at about 8–15 mM, depending on the islet (C. L. Stokes, unpublished data). This suggests that the dependence on V_K in the underlying single cell model is too simplified. The synchronization occurrence and mechanism are not affected, however.

The extracellular volume per cell, v_e, also influences the K_e oscillation size; the concentration of K^+ decreases as v_e increases. To ensure bursting with the assumed value of D (Perez-Armendariz et al., 1985), v_e must be somewhat larger than expected from some electron micrographs that illustrate very narrow, smooth spaces between neighboring β-cells in an islet (e.g., Bonner-Weir (1988)). These micrographs suggest that extracellular volume may be about 1 % of islet volume. In our simulations, this figure is about 8% to keep the oscillations in the range of 2 mM for R = 100 μm. This discrepancy may be explained by the islet vasculature

(Bonner-Weir, 1988) and canalicular spaces (Fujita et al., 1981; Kataoka et al., 1982; Yamamoto and Kataoka, 1984) also seen in electron micrographs. The canalicular spaces among some β-cells are somewhat larger than the spaces between smoothly abutted β-cells. Perivascular space between capillaries and β-cells is also significant. Since most β-cells abut one if not two capillaries (Bonner-Weir, 1988), the total perivascular space may be significant. In addition, because the capillaries are fenestrated, exchange of ions between the extracellular space and intracapillary volume might occur on the burst time scale. For the in vivo or intact perfused pancreas, capillary blood flow may remove some K^+ and minimize accumulation effects if the capillary space is available for K^+ exchange.

3.5 Heterogeneous cell properties

In the spherically symmetric model, when the cells are identical, the outer cells lead and the inner cells lag slightly behind in the burst pattern (Fig. 2). In experiments, Eddlestone et al. (1984) found that interior or exterior cells might lead (personal communication with I. Atwater, regarding Eddlestone et al. (1984)). We find that if all cells do not have the same values of some parameters, the order of bursting can be manipulated. For instance, when f increases linearly (from 0.001 at $r = R$ to 0.002 at $r = 0$), the center and exterior cells burst at about the same time, while the middle cells lag behind (not shown). Since f regulates the burst period, increasing f on the interior shortens the cycle time of those cells, allowing them to catch up to and even lead the exterior cells. This result suggests that the difference between model and experiment may be explained by inhomogeneity of cell properties. Heterogeneity in other parameter values has not been investigated extensively.

3.6. Forcing of burst oscillations

A common feature of many oscillating systems is their susceptibility to entrainment by pulsatile forcing at frequencies different than their natural frequency. We have examined the effects of periodic pulses of increased K^+ in the bath medium at rates both faster and slower than the natural frequency of the islet bursting. One result is illustrated in Fig. 5. The natural burst period of the islet was about 15 s. Two second pulses of 6 mM K^+ in the bath forced the islet to burst with periods as short as 8 s or as long as 20 s. The 1:1, pulse:burst, ratio was lost with either faster or slower forcing. The range of forcing frequencies that can successfully entrain the bursting depends on the size and duration of the pulse, with smaller or briefer pulses being less effective. In laboratory experiments, 2-s pulses of 10 mM K^+ in the perifusion medium at rates faster than the burst frequency could entrain the islet to burst at the pulse frequency, in agreement with the simulations (C. L. Stokes, unpublished data). Entrainment with pulses *less* frequent than the natural frequency was not attempted experimentally, but we conjecture from these calculations that slowing the bursting with such pulses should also be possible.

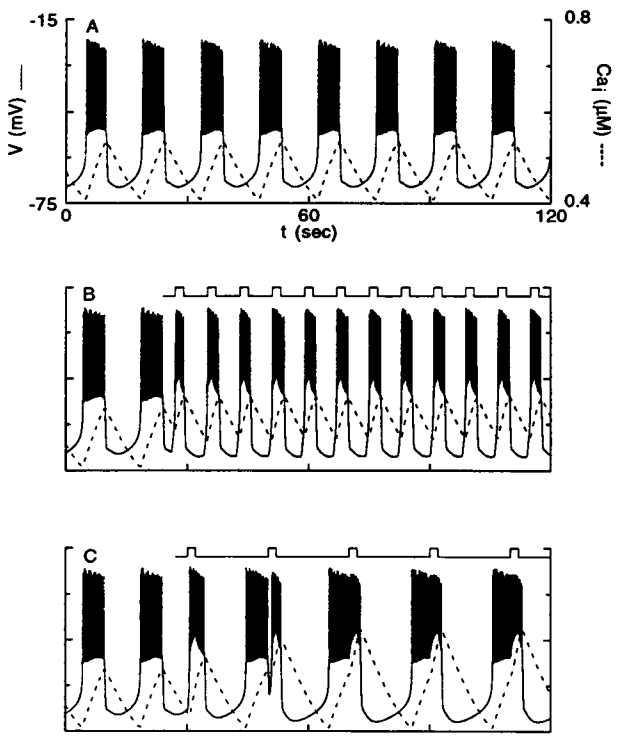

FIGURE 5 Forcing the islet rhythm with periodic pulses of higher K^+ concentration in the bath. (*A*) A normal bursting islet with constant K_{bath} (no forcing), 5 mM K^+. The natural burst period is about 15 s. (*B*) 2-s pulses of 6 mM K^+ in the bath with a period of 8 s can entrain the islet at this same higher frequency. In *B* and *C*, the trace above the burst trajectory represents K_{bath}, illustrating when the steps between 5 and 6 mM were taken. (*C*) 2-s pulses of 6 mM K^+ in the bath with a period of 20 s can entrain the islet to this lower frequency. Frequencies outside the 8–20-s range cannot force the islet in a 1:1 pulse:burst ratio. The outermost bursting cell is illustrated in these figures, and all other cells were in one-to-one synchrony with this cell. The scales in *A–C* are as shown in *A*.

4. DISCUSSION

We have developed a mathematical model of the pancreatic islet of Langerhans to explore the possible role of extracellular K^+ diffusion in the synchronization of electrical bursting among β-cells. Oscillations of K_e in the islet have been measured (Perez-Armendariz et al., 1985; Perez-Armendariz and Atwater, 1986), and experimental manipulation of external K^+ concentration results in burst phase resetting and frequency modulation (Cook et al., 1981; C L. Stokes, unpublished data), demonstrating that K_e significantly affects electrical activity. In our model islet, diffusion of extracellular K^+ results in long-range coupling of electrical activity with synchronization of bursting among cells. The shape and amplitude of the simulated K_e oscillations closely resemble those measured experimentally, supporting the model's diffusion framework. Synchronization occurs even when the K_e oscillations are substantially larger or smaller than those measured experimentally, exhibiting a large range of feasibility of this coupling mechanism.

A significant result of this model is that, for a substantial parameter range, the outer cells lead the inner cells in the burst pattern for spherically symmetric islets. Experiments

indicate that either interior or exterior cells may lead (private communication with Illani Atwater, regarding Eddlestone et al. (1984)). Several factors might account for this difference. First, heterogeneity in burst parameters among cells might influence burst order, as we demonstrated with one parameter. There is evidence for heterogeneity in insulin release rates among β-cells in response to glucose (Stefan et al., 1987). Second, our model ignores electrical coupling via gap junctions and possible stochastic effects of channel opening and closing. Electrical coupling would allow sharing of currents among cells in local areas and might influence burst order. In addition, random channel noise has been shown to prematurely start or end a cell's burst in mathematical models (Sherman and Rinzel, 1991). Finally, asymmetric islet geometry (e.g., elliptical) might affect burst order, because gradients would not be equal in orthogonal directions. Limited simulations with asymmetric three-dimensional structures show some signs of asymmetric burst patterns (not shown).

Synchronization in our model depends on the slow modulation by K_e of the maximum and minimum values of a second slow variable that directly controls the transitions between active and silent phases. Here, the latter slow variable was intracellular calcium concentration, Ca_i, but the synchronization mechanism based on K_e diffusion would also be viable with other slow, negative-feedback variables in any burst paradigm similar to that in Fig. 1 (Chay and Keizer, 1983; Chay, 1987; Chay and Kang, 1988; Sherman et al., 1988; Keizer and Magnus, 1989; Sherman and Rinzel, 1991; Smolen and Keizer, 1992). In fact, we have tested our synchronization mechanism in a simplified system with a different single cell bursting model (Smolen and Keizer, 1992) based on slow voltage feedback on the voltage-dependent calcium channel and ATP-feedback on the K-ATP channel. The bursting becomes synchronized very similar to our results presented here. Recent evidence shows that Ca_i does not vary slowly (Valdeolmillos et al., 1989; Rosario et al., 1990) and that the K-Ca channel may not be very active in β-cell bursting (Kukuljan et al., 1990), suggesting that a different process probably provides the true negative feedback for burst regulation.

Sherman and coworkers (Sherman et al., 1988; Sherman and Rinzel, 1991; Smolen et al., 1993) have modeled the electrical coupling of β-cells with gap junctions. In that case, the membrane potentials of neighboring cells and, therefore, the fast spike-generating dynamics are directly coupled. In our mechanism coupling is indirect; a cell's influence is spread by diffusion through the extracellular medium. The fast dynamics of a cell detect only the localized ionic environment, which changes more slowly than do the membrane variables. As a consequence, we explored synchronization patterns by interpreting the transitions between active and silent phases in terms of a single cell's spiking behavior modulated by two slow variables, Ca_i and K_e, i.e., by using phase diagrams as in Fig. 3. This approach could not be applied to the case of gap junctional coupling, because the coupling is not through a slow variable, and when coupling is weak (Sherman et al., 1988) the transitions are not necessarily understood by parameterizing an uncoupled cell's fast dynamics (see also Rinzel et al., 1992). Finally, a cell can have many neighbors and therefore many direct coupling interactions. With either coupling mechanism one finds parameter regimes where bursting is synchronous but spiking is not. Also, if the model islet is sufficiently large then burst synchrony may give way to wave-like spread of burst activity.

Coupling via gap junctions was not included in our model in order to isolate the effects of K_e on synchronization and demonstrate its feasibility as a coupling mechanism. Since both gap junctions and K_e diffusion are present in islets, both may be involved in synchronization. K_e coupling may synchronize isolated domains of cells coupled tightly by gap junctions within an islet. It could also compensate for incomplete or pathologically weakened gap junctions, although recent simulations (Smolen et al., 1993) with electrical coupling alone show that bursting synchrony survives the loss of up to one-third of neighboring junctions.

The effect of extracellular K^+ on excitable membranes has been explored in other systems. Frankenhaeuser and Hodgkin (1956) measured K^+ buildup in the space surrounding the squid giant axon. The classic Hodgkin-Huxley model (Hodgkin and Huxley, 1952) was subsequently modified by Adelman and Fitzhugh (1975) to account for the effects of K_e accumulation and to better describe firing characteristics, resulting in a better mathematical description of the data. Others have examined the accumulation of K_e during an action potential in various nerve and brain preparations (for review see Spira et al. (1984) and Sykova (1983)). The data indicate that K_e is involved in such conditions as spreading depression (Nicholson and Kraig, 1981), potassium-induced electrographic seizures (Traynelis and Dingledine, 1989), and penicillin-induced epileptogenesis (Swann et al., 1986). Certain nerve cell interactions are even mediated via K_e rather than by chemical or electrotonic synapses (Yarom and Spira, 1981; Spira et al., 1984). K_e also oscillates in beating heart muscle, and the action potential duration decreases during rapid beating, which increases K_e (Kline and Morad, 1978). Several mathematical models investigate the probable roles of extracellular K^+ accumulation and diffusion of various tissues. For instance, Tuckwell and Miura (1978) investigated spreading depression in the cortex, Mathias (1985) studied general syncytial tissues with application to the lens, and Boyett and Fedida (1988) modeled the relationship between heart rate and ion concentrations. In general, these models support the involvement of extracellular K^+ in the function of these tissues. Our present results provide further evidence that extracellular K^+ concentration can significantly affect the function of electrically excitable cells and tissues.

APPENDIX

The steady-state activation curves for the voltage-gated Ca^{2+} and K^+ conductances are given by the following sigmoidal functions:

$$n_\infty(V) = \frac{1}{1 + \exp[(V_n - V)/S_n]} \quad \text{(A1)}$$

$$m_\infty(V) = \frac{1}{1 + \exp[(V_m - V)/S_m]} \quad \text{(A2)}$$

$$h(V) = \frac{1}{1 + \exp[(V - V_h)/S_h]}. \quad \text{(A3)}$$

The time constant curve for the voltage-gated K^+ conductance is given by:

$$\tau_n = \frac{c}{\exp([V - \bar{V}]a) + \exp(-[V - \bar{V}]/b)}. \quad \text{(A4)}$$

In these equations, V_n, V_m, V_h, S_n, S_m, S_h, a, b, c, and $\bar{V}$ are all parameters. Their values were selected by Sherman et al. (1988) to make the equations describe the current-voltage relationships measured by Rorsman and Trube (1986) as well as possible. The values of all parameters are given in Table 1.

TABLE 1 Standard parameter values

Parameter	Definition/first use	Numerical value
K_i (mM)	Intracellular [K^+]; Eq. 5	120
K_{bath} (mM)	[K^+] in bath outside of islet	5
C_m (fF)	Total cell capacitance; Eq. 1	5310
V_{cell} (μm^3)	Cell volume	1150
$\bar{g}_{Ca}$ (pS)	Maximum Ca^{2+} conductance; Eq. 1	1400
$\bar{g}_K$ (pS)	Maximum K^+ conductance; Eq. 1	2500
$\bar{g}_{K\text{-}Ca}$ (pS)	Maximum K-Ca conductance; Eq. 1	30,000
K_d (μM)	Equilibrium constant for Ca^{2+} binding to K-Ca channel; Eq. 3	100
V_{Ca} (mV)	Ca^{2+} reversal potential; Eq. 1	110
k_{Ca} (ms^{-1})	Net Ca^{2+} removal rate; Eq. 3	0.03
f	Fraction of free cytosolic Ca^{2+}; Eq. 3	0.001
F (Coul/mmol)	Faraday's constant; Eq. 4	96.487
RT/F (mV)	Eq. 5	25.0
v_e (μm^3)	Extracellular volume/cell; Eq. 4	100
V_n (mV)	Eq. A1	−15
V_m (mV)	Eq. A2	4
V_h (mV)	Eq. A3	−10
S_n (mV)	Eq. A1	5.6
S_m (mV)	Eq. A2	14
S_h (mV)	Eq. A3	10
a (mV)	Eq. A4	65
b (mV)	Eq. A4	20
c (mV)	Eq. A4	60
λ	Eq. 2	1.6
$\bar{V}$ (mV)	Eq. A4	−75

The authors gratefully thank Dr. Arthur Sherman for many helpful discussions, Drs. Illani Atwater and Eduardo Rojas for laboratory access, and Dr. Jacob Maizel, Chief of the Laboratory of Mathematical Biology, National Cancer Institute, for generously providing computer time and technical support.

C. L. Stokes was supported by a National Research Council-National Institutes of Health Research Associateship.

REFERENCES

Adelman, W. J., Jr., and R. Fitzhugh. 1975. Solutions of the Hodgkin-Huxley equations modified for potassium accumulation in a periaxonal space. *Fed. Proc.* 34:1322–1329.

Ashcroft, F. M., and P. Rorsman. 1989. Electrophysiology of the pancreatic β-cell. *Prog. Biophys. Mol. Biol.* 54:87–143.

Ashcroft, F. M., D. E. Harrison, and S. J. H. Ashcroft. 1984. Glucose induces closure of single potassium channels in isolated rat pancreatic β-cells. *Nature (Lond.).* 312:446–448

Atwater, I., P. Carroll, and M. X. Li. 1989. Electrophysiology of the pancreatic β-cell. *In* Molecular and Cellular Biology of Diabetes Mellitus. Vol. 1. B. Draznin, S. Melmed, and D. LeRoith, editors. Alan R. Liss, New York. 49–68.

Bonner-Weir, S. 1988. Morphological evidence for pancreatic polarity of β-cell within islets of Langerhans. *Diabetes.* 37:616–621.

Boyett, M. R., and D. Fedida. 1988. A computer simulation of the effect of heart rate on ion concentrations in the heart. *J. Theor. Biol.* 132:15–27.

Chay, T. R. 1987. The effect of inactivation of calcium channels by intracellular Ca^{2+} ions in the bursting pancreatic β-cells. *Cell Biophys.* 11: 77–90

Chay, T. R., and H. S. Kang. 1988. Role of single-channel stochastic noise on bursting clusters of pancreatic β-cells. *Biophys. J.* 54:427–435.

Chay, T. R., and J. Keizer. 1983. Minimal model for membrane oscillations in the pancreatic β-cell. *Biophys. J.* 42:181–190.

Chay, T. R., and J. Keizer. 1985. Theory of the effect of extracellular potassium on oscillations in the pancreatic β-cell. *Biophys. J.* 48:815–827.

Chay, T. R., and J. Rinzel. 1985. Bursting, beating and chaos in an excitable membrane model. *Biophys. J.* 47:357–366.

Cook, D. L., and C. N. Hales. 1984. Intracellular ATP directly blocks K^+-channels in pancreatic β-cells. *Nature (Lond.).* 311:271–273.

Cook, D. L., D. Porte, Jr., and W. E. Crill. 1981. Voltage dependence of rhythmic plateau potentials of pancreatic islet cells. *Am. J. Physiol.* 240 (*Endocrinol. Metab.* 3):E290-E296.

Dean, P. M., and E. K. Matthews. 1970. Glucose-induced electrical activity in pancreatic islet cells. *J. Physiol. (Lond.).* 210:255–264.

Doedel, E. 1981. AUTO: a program for the automatic bifurcation analysis of autonomous systems. *Congr. Num.* 30:265–284.

Eddlestone, G. T., A. Gonçalves, J. A. Bangham, and E. Rojas. 1984. Electrical coupling between cells in islets of Langerhans in mouse. *J. Membr. Biol.* 77:1–14.

Frankenhaeuser, B., and A. L. Hodgkin. 1956. The after-effects of impulses in the giant nerve fibres of Loligo. *J. Physiol. (Lond.).* 131:341–376.

Fujita, T., S. Kobayashi, and Y. Serizawa. 1981. Intercellular canalicule system in pancreatic islet. *Biomed. Res.* 2(Suppl.):115–118.

Hodgkin, A. L., and A. F. Huxley. 1952. A quantitative description of membrane current and its application to conduction and excitation in nerve. *J. Physiol. (Lond.).* 117:500–544.

Hopkins, W., L. Satin, and D. Cook. 1991. Inactivation kinetics and pharmacology distinguish two calcium currents in mouse pancreatic B-cells. *J. Membr. Biol.* 119:229–239.

Kataoka, K., M. Yamamoto, T. Yamamoto, and J. Ochi. 1982. Intercellular canalicular system and intercellular junctions in the pancreatic islet of the Mongolian gerbil. *Biomed. Res.* 3:235–238.

Keizer, J., and G. Magnus. 1989. ATP-sensitive potassium channel and bursting in the pancreatic beta cell: a theoretical study. *Biophys. J.* 56: 229–242.

Kline, R. P., and M. Morad. 1978. Potassium efflux in heart muscle during activity: extracellular accumulation and its implications. *J. Physiol. (Lond.).* 280:537–558.

Kukuljan, M., A. A. Gonçalves, and I. Atwater. 1990. Charybdotoxin sensitive K-Ca channel is not involved in glucose-induced electrical activity in pancreatic β-cells. *J. Membr. Biol.* 119:187–195.

Mathias, R. T. 1985. Steady-state voltages, ion fluxes, and volume regulation in syncytial tissues. *Biophys. J.* 48:435–448.

Meda, P., I. Atwater, A. Gonçalves, A. Bangham, L. Orci, and E. Rojas. 1984. The topography of electrical synchrony among β-cells in the mouse islet of Langerhans. *Q. J. Exp. Physiol.* 69:719–735.

Meda, P., R. M. Santos, and I. Atwater. 1986. Direct identification of electrophysiologically monitored cells with intact mouse islets of Langerhans. *Diabetes.* 35:232–236.

Meissner, H. P. 1976a. Electrical characteristics of the beta cells in pancreatic islets. *J. Physiol. (Paris).* 72:757–767.

Meissner, H. P. 1976b. Electrophysiological evidence for coupling between β-cells of pancreatic islets. *Nature (Lond.).* 262:502–504.

Meissner, H. P., and H. Schmelz. 1974. Membrane potential of beta-cells in

pancreatic islets. *Pfluegers Arch. Eur. J. Physiol.* 351:195–206.

Nicholson, C., and R. P. Kraig. 1981. The behavior of extracellular ions during spreading depression. *In* The Application of Ion-Selective Microelectrodes. T. Zeuthen, editor. Elsevier, Amsterdam. 217–238.

Perez-Armendariz, E., and I. Atwater. 1986. Glucose-evoked changes in $[K^+]$ and $[Ca^{++}]$ in the intercellular spaces of the mouse islet of Langerhans. *In* Biophysics of the Pancreatic β-Cell. I. Atwater, E. Rojas, and B. Soria, editors. Plenum Publishing Corp., New York. 31–51.

Perez-Armendariz, E., E. Rojas, and I. Atwater. 1985. Glucose-induced oscillatory changes in extracellular ionized potassium concentration in mouse islets of Langerhans. *Biophys. J.* 48:741–749.

Perez-Armendariz, E., C. Roy, D. C. Spray, and M. V. L. Bennett. 1991. Biophysical properties of gap junctions between freshly dispersed pairs of mouse pancreatic beta cells. *Biophys. J.* 59:76–92.

Plant, T. D. 1988. Properties and calcium-dependent inactivation of calcium currents in cultured mouse pancreatic B-cells. *J. Physiol. (Lond.).* 404: 731–747.

Prentki, M., and C. B. Wollheim. 1984. Cytosolic free Ca^{2+} in insulin secreting cells and its regulation by isolated organelles. *Experientia (Basel).* 40:1052–1060.

Rinzel, J. 1985. Bursting oscillations in an excitable membrane model. *In* Ordinary and Partial Differential Equations. B. D. Sleeman and R. J. Jarvis, editors. Springer-Verlag, New York. 304–316.

Rinzel, J., A. Sherman, and C. L. Stokes. 1992. Channels, coupling, and synchronized rhythmic bursting activity. *In* Analysis and Modeling of Neural Systems. F. Eeckman, editor. Kluwer Academic Publishers, Boston. 29–46.

Robinson, R. A., and R. H. Stokes. 1959. Electrolyte solutions. Butterworths, London.

Rorsman, P., and G. Trube. 1986. Calcium and delayed potassium currents in mouse pancreatic β-cells under voltage clamp conditions. *J. Physiol. (Lond.).* 374:531–550.

Rosario, L. M., R. M. Santos, D. Contreras, B. Soria, and M. Valdeolmillos. 1990. Glucose-induced oscillations of intracellular Ca^{2+} and membrane potential in single mouse islets of Langerhans. *Biophys. J.* 57:306*a*. (Abstr.)

Satin, L. S., and D. L. Cook. 1989. Calcium current inactivation in insulin-secreting cells is mediated by calcium influx and membrane depolarization. *Pfluegers Arch. Eur. J. Physiol.* 404:385–387.

Sherman, A., and J. Rinzel. 1991. Model for synchronization of pancreatic β-cells by gap junction coupling. *Biophys. J.* 59:547–559.

Sherman, A., J. Rinzel, and J. Keizer. 1988. Emergence of organized bursting in clusters of pancreatic β-cells by channel sharing. *Biophys. J.* 54: 411–425.

Smolen P., and J. Keizer. 1992. Slow voltage-inactivation of Ca^{2+} currents and bursting mechanisms for the mouse pancreatic beta-cell. *J. Membr. Biol.* 127:9–19.

Smolen P., J. Rinzel, and A. Sherman. 1993. Why pancreatic islets burst but single β-cells do not: the heterogeneity hypothesis. *Biophys. J.* 64:1668–1680.

Spira, M. E., Y. Yarom, and D. Zeldes. 1984. Neuronal interactions mediated by neurally evoked changes in the extracellular potassium concentration. *J. Exp. Biol.* 112:179–197.

Stefan, Y., P. Meda, M. Neufeld, and L. Orci. 1987. Stimulation of insulin secretion reveals heterogeneity of pancreatic β-cells in vivo. *J. Clin. Invest.* 80:175–183.

Swann, J. W., K. L. Smith, and R. J. Brady. 1986. Extracellular K^+ accumulation during penicillin-induced epileptogenesis in the CA_3 region of immature rat hippocampus. *Dev. Brain Res.* 30:243–255.

Sykova, E. 1983. Extracellular K+ accumulation in the central nervous system. *Prog. Biophys. Mol. Biol.* 42:135–189.

Traynelis, S. F., and R. Dingledine. 1989. Role of extracellular space in hyperosmotic suppression of potassium-induced electrographic seizures. *J. Neurophysiol. (Bethesda).* 61:927–938.

Tuckwell, H. C., and R. M. Miura. 1978. A mathematical model for spreading cortical depression. *Biophys. J.* 23:257–276.

Valdeolmillos, M., R. M. Santos, D. Contreras, B. Soria, L. M. Rosario. 1989. Glucose-induced oscillations of intracellular Ca^{2+} concentration resembling bursting electrical activity in single mouse islets of Langerhans. *FEBS Lett.* 259:19–23.

Wollheim, C. B., and G. W. G. Sharp. 1981. The regulation of insulin release by calcium. *Physiol. Rev.* 61:914–973.

Yamamoto, M., and K. Kataoka. 1984. A comparative study on the intercellular canalicular system and intercellular junctions in the pancreatic islets of some rodents. *Arch. Histol. Jpn.* 47:485–493.

Yarom, Y., and M. E. Spira. 1981. Extracellular potassium ions mediate specific neuronal interaction. *Science (Wash. DC).* 216:80–82.